Chapter VI

As there is an increasing thrust towards the development of new drugs for curing and detecting the fatal diseases such as cancer, HIV etc., The medicinal and photophysical application of metal complexes particularly transition metals are excellent due to their variable oxidation states, range of coordination numbers and tuning ability according to the need and they are more potential than organic-based drugs. [1-4]

The d^6 complexes such as Ir(III) exhibit excellent photophysical and pharmacological applications because they are chemically inert and due to slow exchange of ligands, these complexes act as therapeutic and bioimaging reagents for cellular applications.[5]

Pt(IV) compound satraplatin underwent phase III clinical trials for the treatment of hormone-refractory prostate cancer[6] and other examples such as osmium complexes[7] are promising for addressing the problem of intrinsic or acquired resistance in chemotherapy, a cobalt-alkyne analogue of the anti-inflammatory drug.[8]

The hitherto synthesised ligands and complexes were selectively subjected to various *in silico*, *in vitro* pharmacological studies and photophysical studies.

6.1.1. *In silico* studies

The biological importance of the synthesised ligands and the complexes were predicted theoretically by using DFT/B3LYP functional d,p basis set. The molecular electrostatic potential (MEP) analysis of the compounds is shown below **Fig (201-208)**. The active site of the complexes is indicated in color. From the results, it was inferred that the maximum surface of the complexes may act as a binding site.

14a

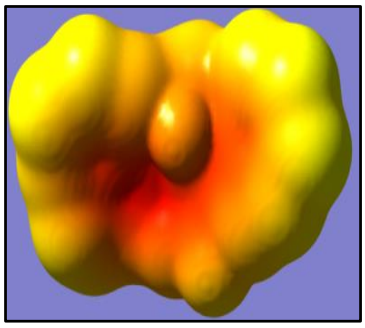

15a

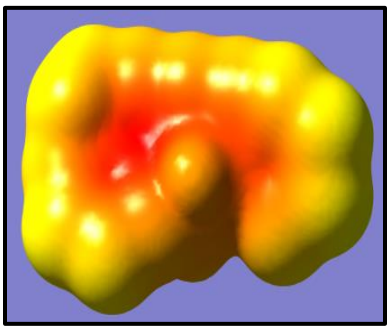

16a

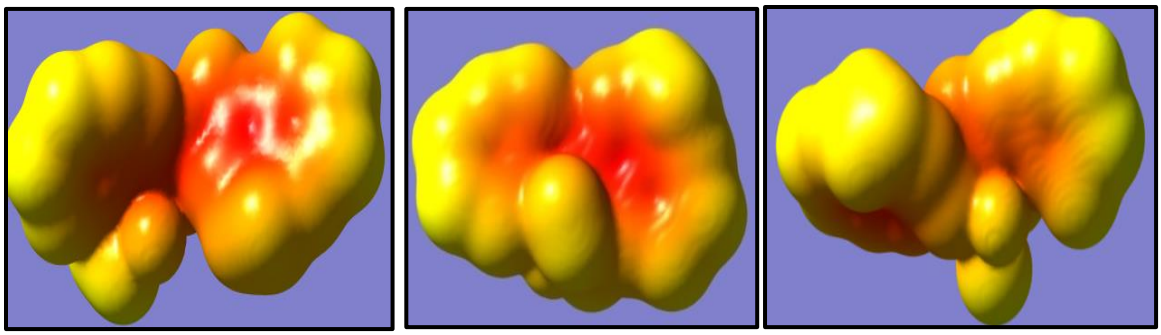

17a **18a** **19a**

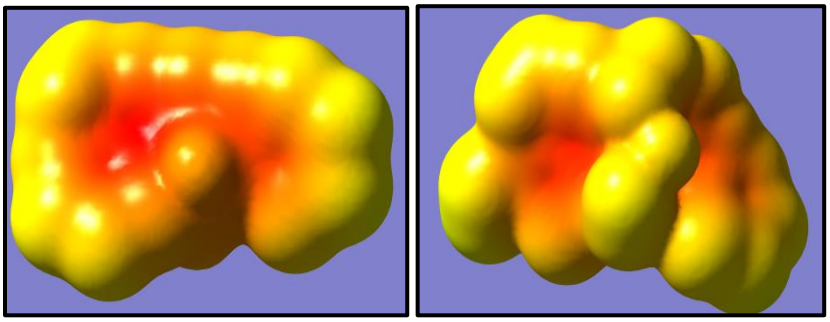

20a **21a**

Fig (201-208) - MEP diagram of complex (14a-21a)

6.1.2. ADMET Property

Satisfying and obeying the ADMET property, is the prime criteria for a molecule to act as a drug. Hence the ligands synthesised were subjected to ADMET property using Molsoft's chemical fragments in order to validate their drug likeness property. **Fig (211-218).**

Table 19: The value of log P & log S of ligand 11(a-d) & 13(a-d)

Compound	HBA	HBD	log P	log S	Drug-likeness score
11a	3	2	4.42	-5.03	-0.43
11b	3	2	4.82	-5.36	-0.49
11c	3	2	4.69	-5.35	-0.17
11d	4	2	4.51	-5.18	-0.08
13a	4	3	3.99	-6.22	-0.11
13b	4	3	3.99	-6.22	-0.18
13c	3	3	5.20	-6.99	**-0.01**
13d	4	3	4.57	-6.24	-0.09

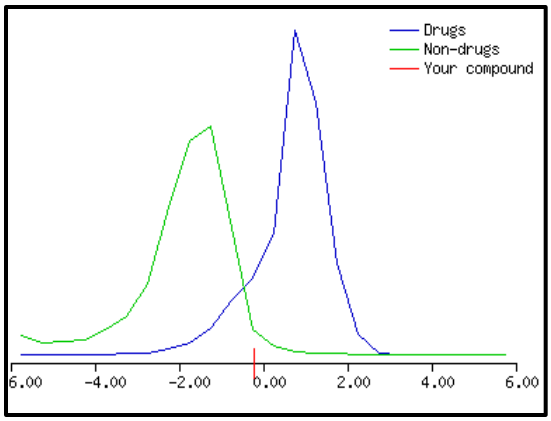

Fig (209) ligand 11a

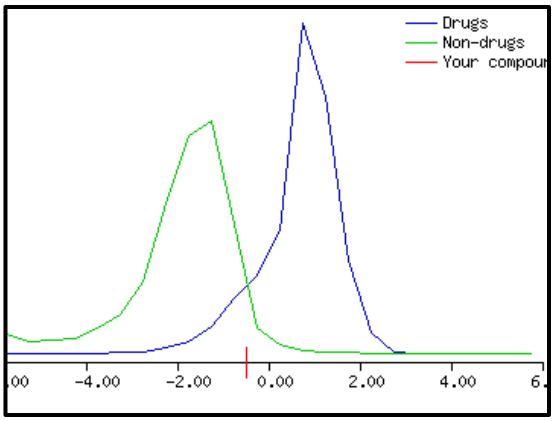

Fig (210) ligand 11b

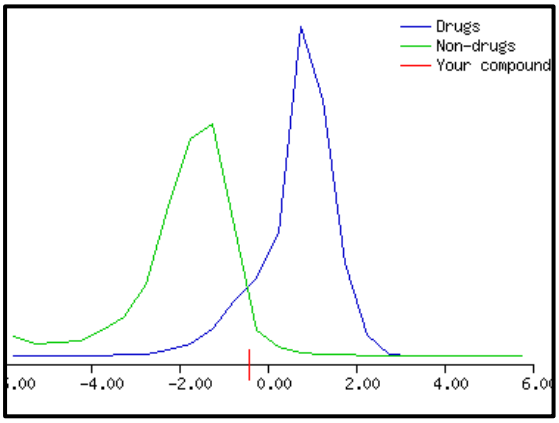

Fig (211) ligand 11c

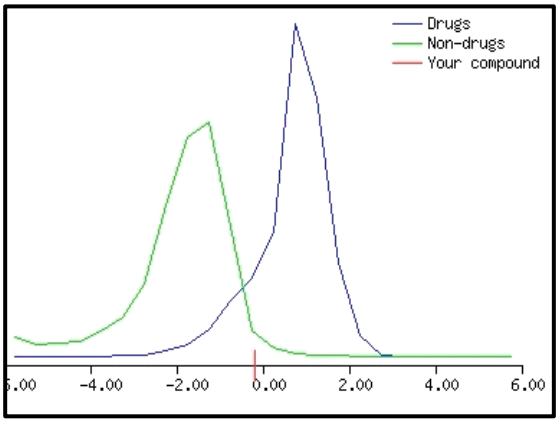

Fig (212) ligand 11d

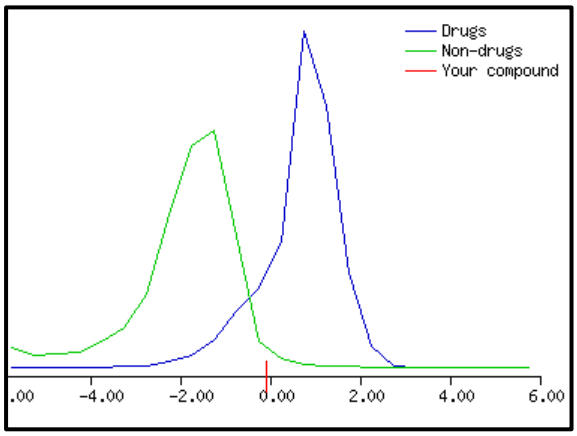

Fig (213) ligand 13a

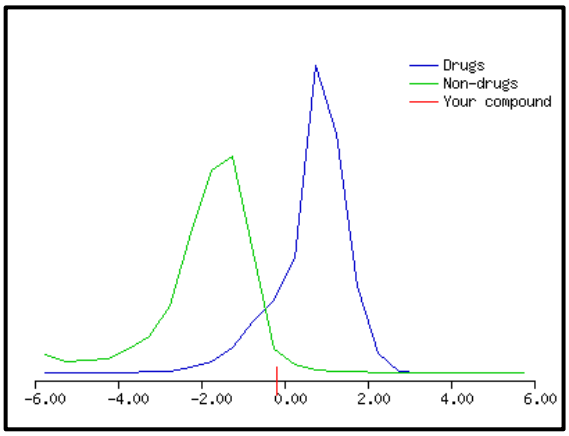

Fig (214) ligand 13b

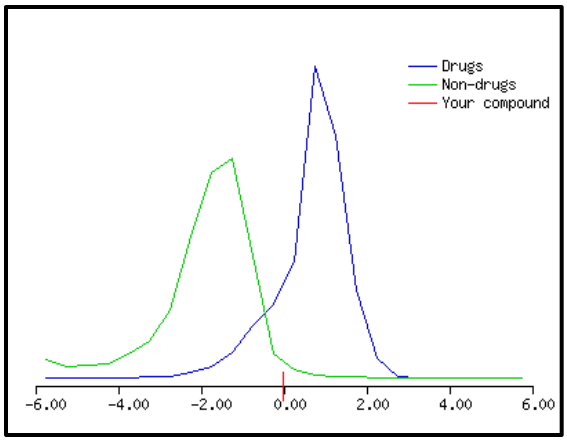

Fig (215) ligand 13a

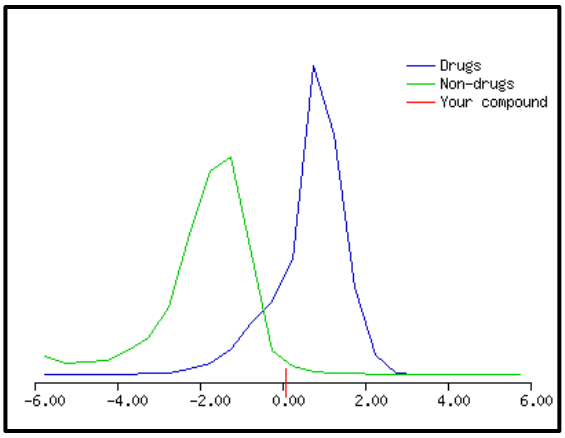

Fig (216) ligand 13b

From the above results, the ligands are found to be well in line with the drug and the ligands possessing thiosemicarbazino system of methoxy and chloro are found to be prominent drugs when compared to other compounds.

After checking the drug likeness score, few of the selected ligands and the complexes **(iridium(III) & osmium(III))** were subjected to the docking studies using Autodock 4.0 tool.[9,10]

6.1.3. Molecular docking

Human epidermal growth factor receptor was downloaded from Protein Data Bank (PDB) with the following PDB ID: 2ITY. Docking analysis was performed by Autodock4.0 tool.

Protein and the ligand were prepared for docking analysis with MGL Tool 1.5.6. Grid box was prepared as X=56, Y=68, Z=54 with grid-point spacing angstrom of 0.858Å. The X, Y, Z coordinates were specified for grid point value of X= -58.166, Y= -5.006, Z= -21.212 and total grid points per map of 216315 were constructed enveloping the human epidermal growth factor receptor. The given input parameters were analyzed using a genetic algorithm and set 100 runs for each docking process. Finally, the best conformation was selected with the lowest binding energy, ligand efficiency, with more number of hydrogen bonds.

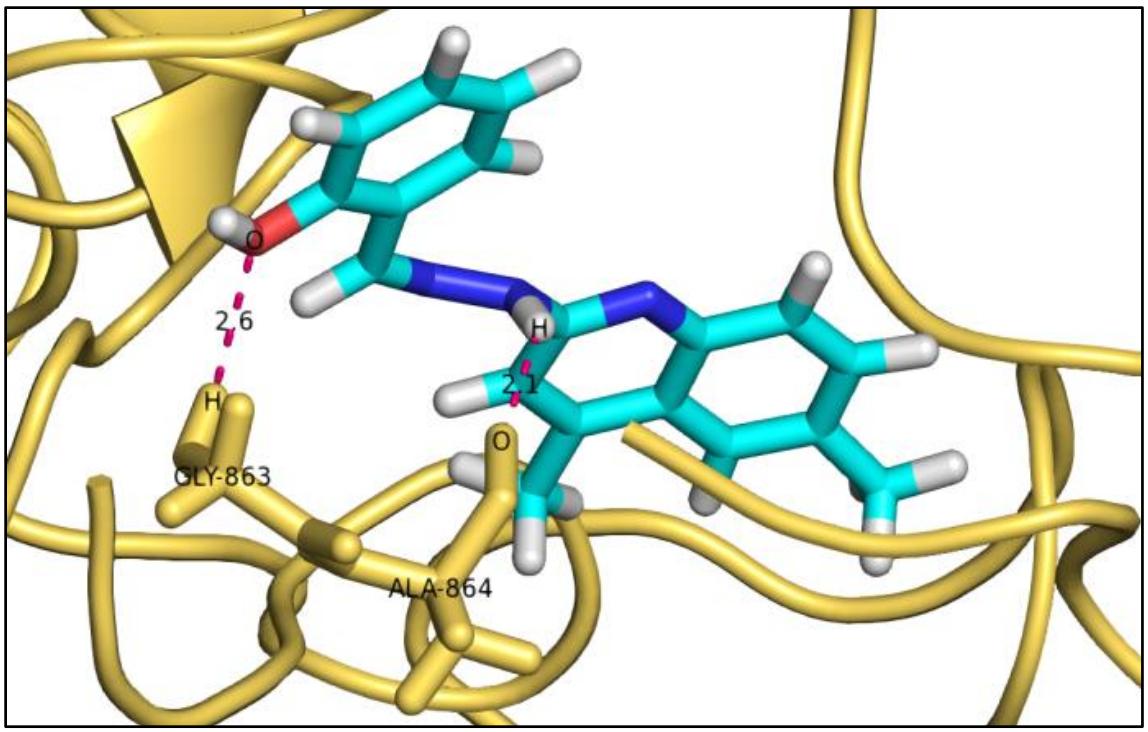

Fig 217 - Docking pose of ligand 11b

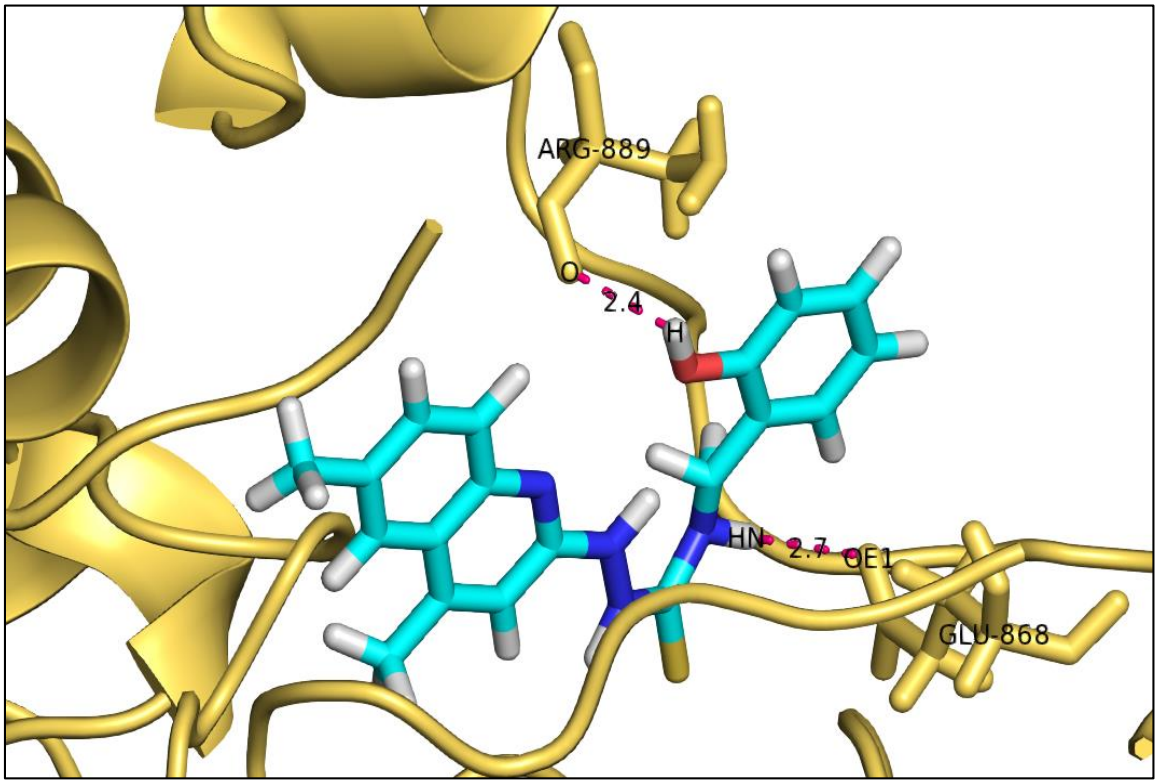

Fig 218 - Docking pose of ligand 13b

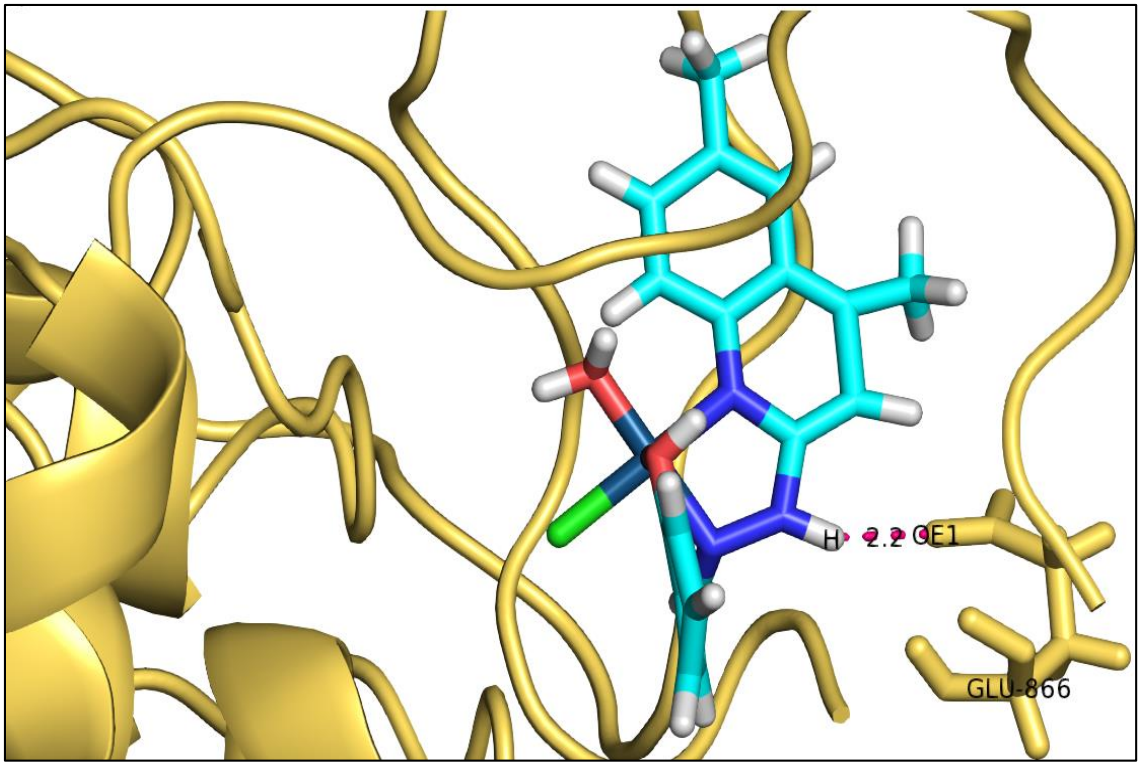

Fig 219 - Docking pose of iridium (III) complex 14b

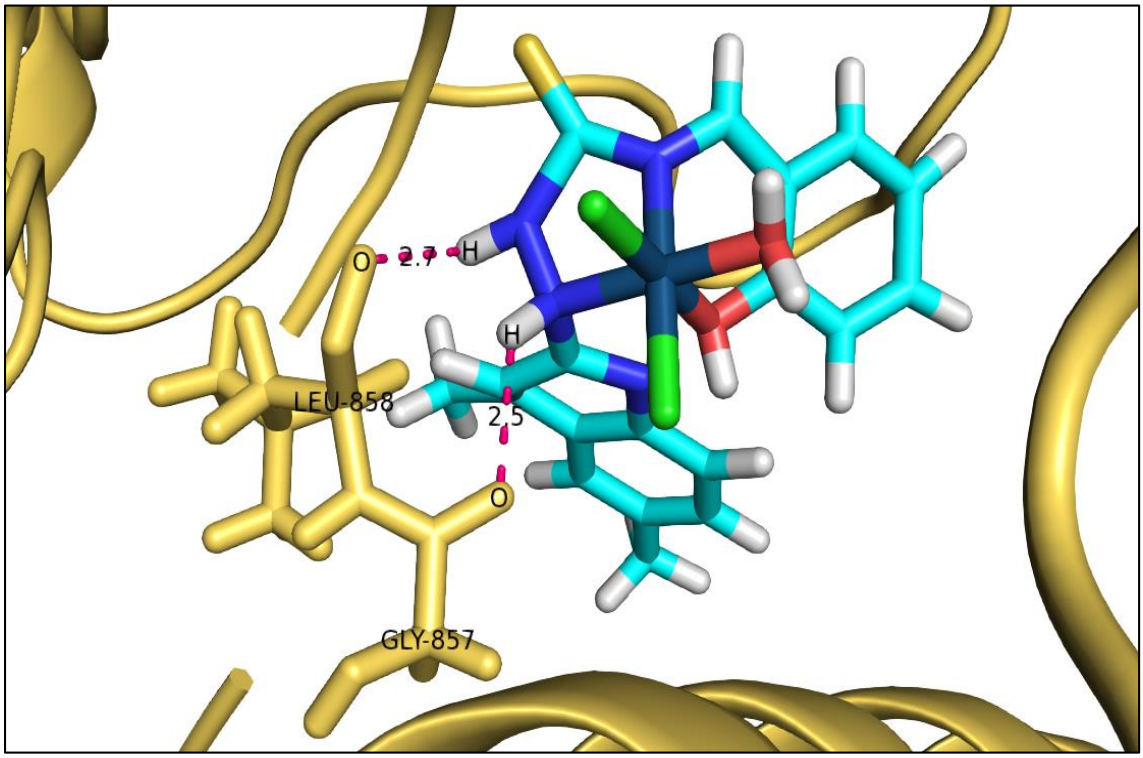

Fig 220 - Docking pose of iridium (III) complex 15b

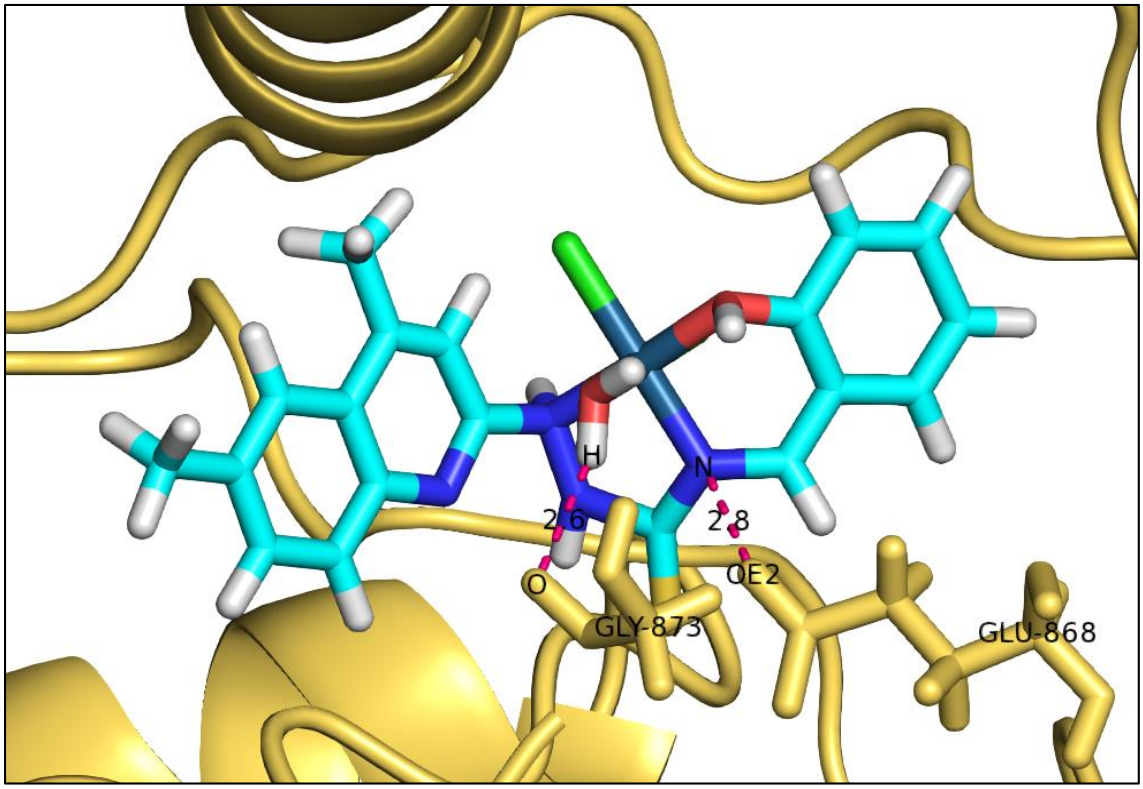

Fig 221 - Docking pose of osmium (III) complex 18b

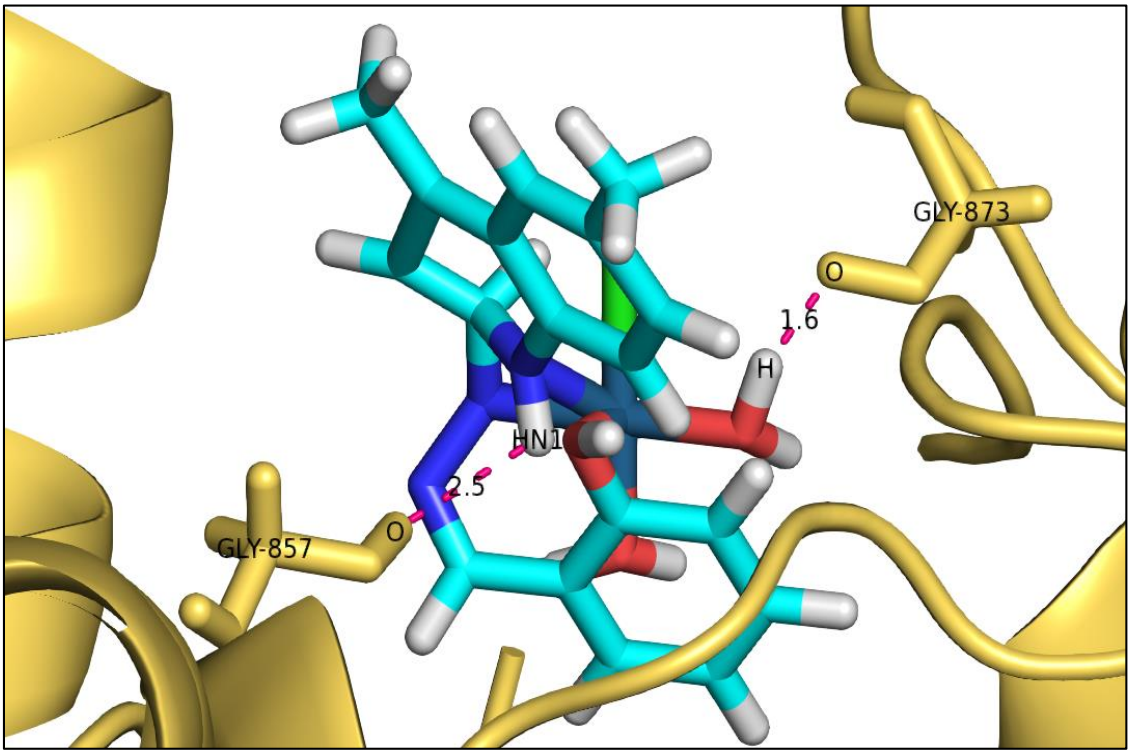

Fig 222 - Docking pose of osmiuum (III) complex 19b

The graphical representation of human epidermal growth factor receptor interacted with synthetic compounds (**11b, 13b, 14b, 15b, 18b** and **19b**). Receptor interactions with ligand are representing by yellow orange, cyan and magenta colors respectively. **Fig (11b)** shows atomic interaction between hydrogen, oxygen atoms of GLY863, ALA864 and oxygen, hydrogen atoms of **(11b)** compound. **Fig (13b)** shows atomic interaction between OE1, oxygen atoms of GLU868, ARG889 and HN, oxygen atoms of (**13b)** compound. **Fig (14b)** shows atomic interaction between OE1 atom of GLU866 and hydrogen atom of (**14b)** compound. **Fig (15b)** shows atomic interaction between oxygen's atoms of GLY857, LEU858 and hydrogen's atoms of **15b** compound.

Fig (18b) shows atomic interaction between oxygen's atoms of GLY857, GLY873 and HN1, hydrogen atoms of (**18b)** compounds. Fig (**19b)** shows atomic interaction between OE2, oxygen atoms of GLU868, GLY873 and nitrogen, hydrogen atoms of (**19b)** compound.

Molecular docking studies of human epidermal growth factor receptor with synthetic compounds (**11b, 13b, 14b, 15b, 18b, 19b,**) were analyzed for the lowest binding energy, lowest ligand efficiency and more than number of hydrogen bonds were formed for the best interaction. The length of bond distance between the receptor and ligand below **3Å** is the best.

The selected synthetic compounds docked with human epidermal growth receptor and it showed interactions within the limits of **3Å**

Table 20 summarizes the results obtained

Table 20: Interaction of synthetic compounds with human epidermal growth factor receptor

Compounds	Binding energy (Kcal/mol)	Ligand efficiency (Kcal/mol)	Hydrogen bond interaction residues with atoms	Distance between residues (Å)
11b	-5.26	-0.24	GLY863:H:O; ALA864:O:H	2.6 2.1
13b	-5.5	-0.22	GLU868:OE1:HN; ARG889:O:H	2.7 2.4
14b	-6.17	-0.21	GLU866:OE1:H	2.2
15b	-7.04	-0.23	GLY857:O:H; LEU858:O:H	2.5 2.7
18b	-7.33	-0.28	GLY857:O:HN1; GLY873:O:H	2.5 1.6
19b	-6.98	-0.24	GLU868:OE2:N; GLY873:O:H	2.8 2.6

With the continuation of the above theoretical perceptions, we have carried out the pharmacological results for the compounds containing methoxy substituents (electron donating system) and chloro compounds (electron withdrawing sustituemts) and the results are summarized.

6.1.4. Antimicrobial activity (Well diffusion method)

Antibacterial and antifungal activities were studied by Well diffusion method following the literature procedure.[11]

6.1.4.1. Antibacterial Activities

Antibacterial activities of the iridium (III) and osmium (III) complexes **14c, 15c, 14d, 15d, 18c, 18d, 19c** and **19d** were studied against the bacteria *Staphylococcus aureus (S.a), Bacillus cereus (B.c), Micrococcus luteus (M.l), Escherichia coli (E.c), Pseudomonas aeruginosa (P.a)*.at a concentration 100µg/L. Gentamycin was used as the standard for antibacterial studies. The media for antibacterial study is nutrient agar (NA).

6.1.4.2. Antifungal Activities

Antifungal activities of the synthesized complexes **14c, 15c, 14d, 15d, 18c, 18d, 19c** and **19d** were studied against the fungals *Candida albicans, Aspergillus flavus and Fusarium sp*. at a concentration 100µg/L. Clotrimazole was used as the standard for antifungal studies. The media for antifungal study is potato dextrose agar (PDA).

Antibacterial Activity

The values of inhibition zone in mm of various metal complexes are tabulated as follows **(Table-21).**

Table 21: The value of inhibition Zone of metal complexes in mm

Different bacterias	The inhibition Zone of metal complexes in mm (100µg/L)								
	14c	**14d**	**18c**	**18d**	**15c**	**15d**	**19c**	**19d**	**Standard**
Staphylococcus aureus	14	11.5	15.3	15	15.4	15.1	15.8	15.5	16.2
Bacillus cereus	12.5	10.5	14.8	14	14.2	13.8	14.7	14.8	15.8
Micrococcus luteus	11.5	11	12	11.9	12.2	11.8	13.4	13.1	13.75
Escherichia coli	10	6	11	12	11.5	10.4	11.8	11.2	13.25
Pseudomonas aeruginosa	5	11	7.2	8.8	8.2	9.5	7.4	7.6	11.5

It was found that the complexes were active against *Staphylococcus* aureus, and *Micrococcus luteus (M.l),* and is almost equal to the standard gentamycin. The complexes were less active against *Pseudomonas aeruginosa* when compared to the standard.

Among the complexes studied for the antibacterial activity, the chloro and methoxy substituted thiosemicarbazone ligands possess higher activity than their corresponding hydrazino derivatives. Also, it was noticed that the other substituted ligands are found to be less active when compared to **15c, 15d, 19c** and **19d**.

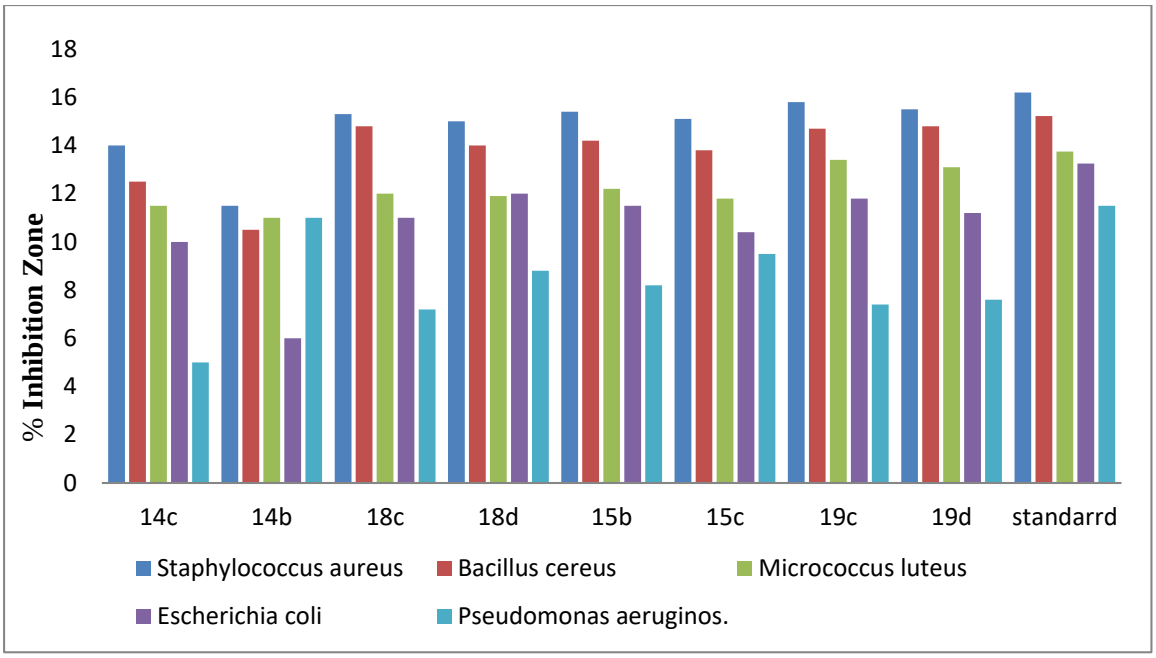

Fig 223 - Metal complexes 14c, 15c, 14d, 15d, 18c, 18d, 19c and **19d**

The MIC of the platinum complexes **(16b, 16c, 16d, 17b, 17c** and **17d)** and cobalt complexes (**20a, 20b, 20c, 21a, 21b** and **21c**) were subjected to antibacterial activities against the bacteria *E.coli, B.subtilis and S.aureus* and are tabulated in **Table-22.**

Table 22: MIC values of Pt(IV) and Co(II) complexes

S.No	Sample code/ complex No	E.coli	B.subtilis	S.aureus
		MIC (mg/mL)		
1.	16b	16.66	50.00	27.50
2.	16c	33.33	25.55	27.50
3.	16d	8.33	16.00	15.60
4.	17b	0.13	3.12	3.90
5.	17c	16.66	25.55	13.75
6.	17d	14.48	22.5	12.24
7.	20b	66.66	25.44	22.80
8.	20c	16.66	6.25	13.70
9.	20d	16.66	25.55	13.70
10.	21b	66.66	25.55	55.00
11.	21c	33.33	12.50	45.80
12.	21d	4.16	6.25	1.90
13.	Standard	1.58	2.3	2.9

The Minimum Inhibitory Concentrations value of complex **17b** was found to be greater than the standard when compared to other complexes against all the three bacteria studied. Further, the order of MIC value are found to be

21d> 16d> 17d> 17c> 16b= 20c= 20d> 16c= 21c> 20b= 21b

Antifungal Activity

The value of inhibition zone in mm of various metal complexes **15c, 17c, 19c** and **21c** are tabulated as follows **(Table 23)**

Table 23: The value of inhibition zone in mm

Fungus studied	Inhibition zone in mm (100µg/mL)				
	15c	**17c**	**19c**	**21c**	**Standard**
Candida albicans	12.5	14.8	11.5	14.5	17
Aspergillus flavus	8	10	8	9	21.5

It was found that the complexes were active against *Candida albicans* and *Aspergillus flavus.* The activity against *Candida albicans* values is almost equal to the standard value.

On comparing the antimicrobial activity of the compounds studied,it was found that the compound **15c,17c,19c and 21c** shows higher activity which also in line with the ADMET scores**.**

The order of activity among the complexes studied is as shown

Pt(IV)> Co(II)> Ir(III)> Os(III)

6.1.5. Antioxidant activity

The newly synthesized Schiff base and its metal complexes **11c, 13c, 15c, 17c, 19c** and **21c** were screened for free radical scavenging activity using 2,2-diphenyl-1-picryl-hydrazyl-hydrate (DPPH) assay. The results of the free radical scavenging activity of the compounds at different concentrations are shown in (**Table 24)**. It is evident from the results that the free radical scavenging activity of these compounds was concentration dependent.

The order of the minimum inhibitory concentration of the complexes and ligand

17c > 21c > Std > 19c > 15c > 13c > 11c

Among the examined metal complexes, the higher activity of the complexes in comparison with the ligand could be high due to the coordination of metal with azomethine nitrogen and phenolic oxygen of the ligand.

Table 24: The values of inhibition zone of metal complexes 11c, 13c, 15c, 17c, 19c and 21c

Concentration In µg/mL	Standard	Complex 11c	Complex 13c	Complex 15c	Complex 17c	Complex 19c	Complex 21c
20	33.44	18.88	20.08	39	44.89	32.44	31.85
40	34.24	24.52	25.85	44	52.94	33.21	51.70
80	58.61	26.78	27.54	54	62.81	44.65	64.62
100	74.48	27.98	29.7	57	71.42	56.85	67.68
200	80.02	30.97	30.59	62.08	74.48	72.25	75.28
IC 50	65.8	>100	>100	78.2	37	76.4	38.5

The enhanced activity of the complexes over the ligand can be explained on the basis of chelation theory. It is observed that, in a complex, the positive charge of metal is partially shared with the donor atoms present in the ligand and there may be π-electron delocalization over the whole chelation. The increase in the lipophilic character of the metal chelate, favors its permeation through the lipoid layer of the bacterial membranes. Therefore all the metal complexes exhibited higher activity than ligand **11a** and **13a.**

On comparing the metal complexes, platinum (IV) and cobalt (II) complexes exhibit higher activity than Ir(III) and Os(III) complexes.

6.1.6. Cytotoxicity studies

The anticancer activity of the synthesized compounds was carried out against HeLa cancer cell line that may act through EGFR TK inhibition by MTT assay method. This method is used to determine either the percentage of cell viability or cell death.

The cell line was cultured and preserved in DMEM medium along with antibiotics in a T-shaped flask, kept in incubator chamber at 37.5 ^{o} C with 5% CO_2 for 24-72 h. The samples and control were prepared in different concentrations with 1mg/1mL stock solutions and by using micropipette, the samples, controls and cell line were filled in the plates with cultured cell lines. After mixing well, the plate was kept for 24 h in 5% CO_2 incubator. After incubation, wash the cells were washed with trypsin then MTT dye was added to the cells in the plate. Then again it was incubated for 24 h in 5% CO_2 atmosphere. Thereafter the optical density value was monitored from ELISA reader at 570 nm.

$$\% \text{ of cell death} = \frac{(\text{control OD value} - \text{sample OD value})}{\text{control OD value} \times 100}$$

Cellular level *in vitro* cytotoxicity studies were carried out against HeLa cancer cell line for four of the iridium complexes (**14c and 15c)** and platinum complexes (**16c and 17c)** compared with the standard drug cisplatin. The stock solutions of the samples were prepared by the concentration (1 mg / l mL) and distributed in the cells as 10 μL, 20 μL and 30 μL and followed the procedure and experiment was carried in triplicates.

The potency was found to vary for different functional groups of the sample. Complex (**16c)** exhibits 50 % cell death at the concentration very close to the standard. The order of % cell death is

Cisplatin > Complex 16c > Complex 14c > Complex 17c > Complex 15c

The comparative analysis of cytotoxic activity of compounds with cisplatin was conducted in order to better understand their pharmacological behavior. The two–Cl groups in cisplatin are responsible for their pharmacokinetics, as same in the case of our compounds.

The electronic effect on the metal coordinated ligand might influence the strength of M-C, M-O and M-N bond as well as the rate of hydrolysis which inturn affects the anticancer activity of the complex as mentioned.

Table 25 - % of cell death of various complexes against HeLa cancer cell line

Samples	Concentration in 10^{-3}(µL) Replications	% Cell Death			IC_{50} in (µL)
		10	20	30	
14c	I	46.59	51.5	52.23	19.62
	II	46.05	50.99	52.31	
	III	47.31	52.01	57.56	
15c	I	15.29	26.05	40.44	38.08
	II	15.11	26.67	40.45	
	III	15.12	26.46	40.74	
16c	I	58.88	63.48	68.07	9.32
	II	58.69	63.45	68.69	
	III	59.49	64.19	69.01	
17c	I	26.66	40.45	47.08	31.86
	II	27.21	40.57	46.71	
	III	27.72	40.56	46.53	
Cisplatin	I	52.53	60.21	68.5	6.959
	II	52.49	60.62	68.69	
	III	52.50	60.51	68.71	

The compounds **14c, 15c, 16c and 17c** were analyzed, the structure of metal complexes having the chelated system (ie) NNO and NOS fashion, which stabilize the compounds. The two –Cl groups present in the compound leads to fast reduction and high toxicity. On comparing with the standard, the compounds **14c, 15c and 17c** are more cytotoxic towards the cell lines than standard and the compound **16c** showed more or similar activity of standard because in the platinum(IV) complexes, presence of two chlorine groups and a hydrazino moiety would enhance the pharmacodynamic property.

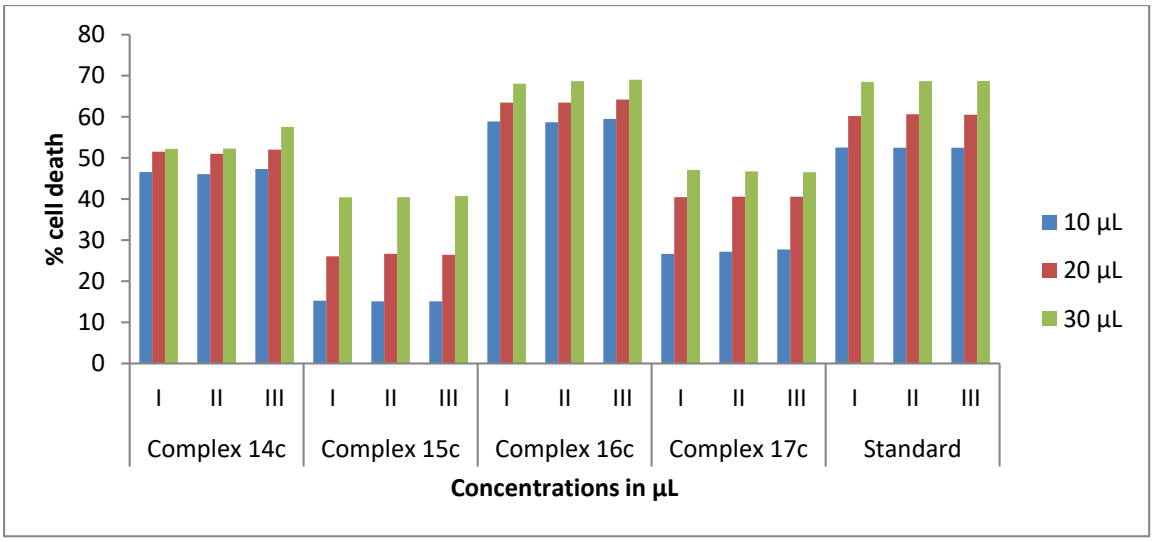

Fig 224 – Histogram images of % of Cell death of 14c, 15c, 16c and 17c

6.1.7. DNA cleavage studies

DNA cleavage study was performed using DNA nicking assay, 2 µL of the sample was added to 5 µL of plasmid DNA (PBR322) along with 2 µL of hydrogen peroxide. After addition, the sample was incubated for 1 hour at 37 ^{o}C. Later the sample was run in agarose gel natural action. To the 1.2 % agarose gel, along with DNA ladder (Biolab) all the sample were loaded separately and run at 50V. The results were recorded using a UV transilluminator and documented.

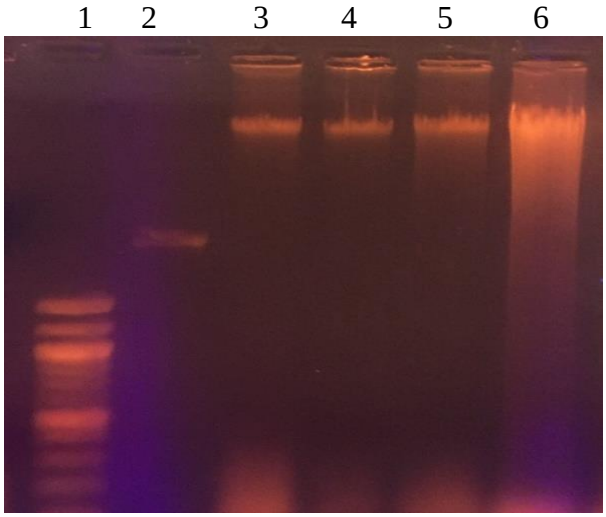

Lane 1: Marker (1kb Ladder)

Lane 2: Control DNA

Lane 3: 14c + DNA

Lane 4: 15c + DNA

Lane 5: 16c + DNA

Lane 6: 17c + DNA

Fig 225 - DNA cleavage of various lanes of metal complexes

Investigations of interaction of DNA with small molecules are basic in the design of new drug in the field of pharmaceutical chemistry. Some metal complexes interact with DNA and induce the breakage of DNA strands and thus cancer genes, after DNA strand cleaves, the DNA double strands break the replication ability of the cancer gene is destroyed.

To access the DNA cleavage ability of the metal complexes **14c, 15c, 16c and 17c,** supercoiled plasmid DNA (PBR322) along with hydrogen peroxide was incubated for 1 h at 37 ^{o}C. Later the sample was run in agarose gel medium. To the 1.2 % agarose gel, along with DNA ladder (Biolab) all the sample were loaded separately and run at 50V. Then the DNA cleavage was examined.

The study revealed that all the complexes damaged the DNA and produced the smeared DNA while running on 1.2% agarose gel.

General mechanism proposed for DNA cleavage by hydroxyl radicals is oxidative (ie) abstraction of hydrogen from sugar units predict the release of specific residues arising from transformed sugars, depending on the position from which the hydrogen is removed. The cleavage is repressed by the free radical hunters suggesting that hydroxyl radicals facilitate the cleavage.

6.1.8. Photophysical Studies

6.1.8.1. Emission Spectra

The emission spectra of the iridium complexes **14 and 15** and platinum complexes **16 and 17** in the concentration of 10^{-5} were carried out in ethanol medium at room temperature. The emission spectra of all these complexes show similar emission in the wavelength range of 465-470 nm. From the data it is clear that the complexes containing electron withdrawing group and having extensive conjugation will be highest emission intensity compared to other complexes.

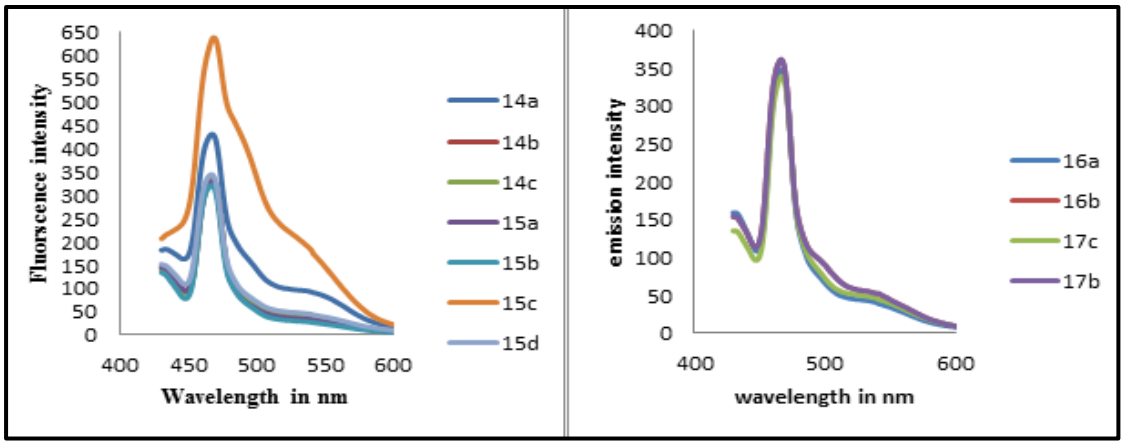

Fig 226- Emission spectra of Ir(III) and Pt(IV) complexes

Complexes **15c** and **17c** showed highest intensity (at 638, 468 nm and 362, 467 nm respectively) when compare to other complexes. This might be due to the presence of electron withdrawing substituents. A hyperchronic shift is noted in the thiosemicarbazones complexes.

6.1.8.2. Photoluminescent Spectra

The photoluminescence (PL) spectrum of the iridium, platinum and cobalt complexes was performed in spectrofluorimeter 350W Xe lamp as the excitation source.

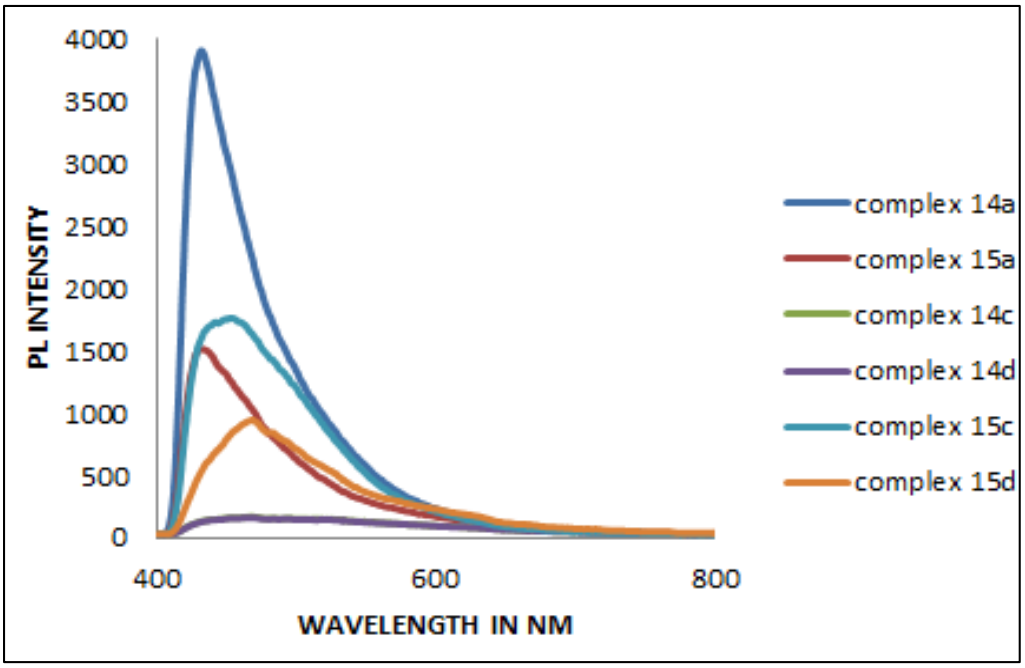

Fig 227- PL spectra of Ir(III) complexes

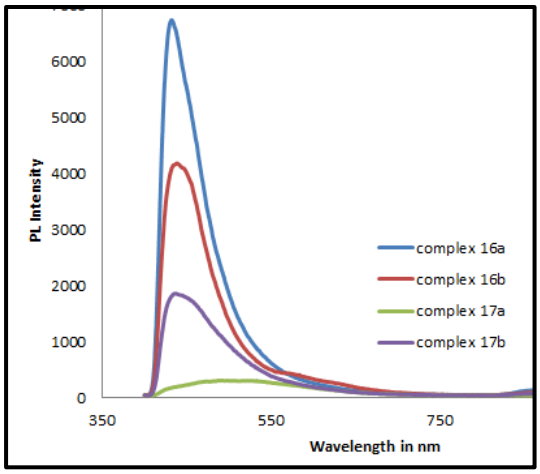

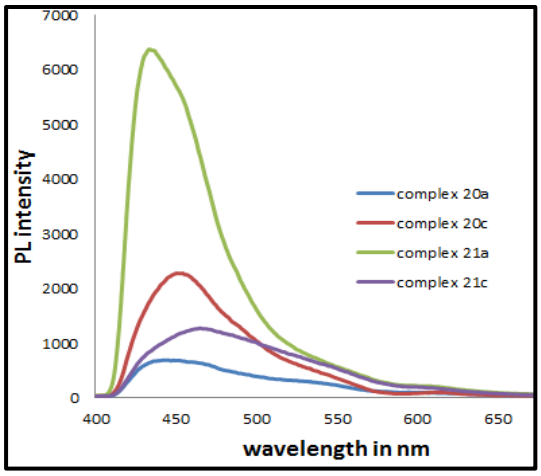

Fig 228 & 229 - PL spectra of Pt(IV) & Co(II) complexes

Different λ_{max} and intensity values obtained for the complexes **(14a-21c)** are tabulated in **Table - 26**

Table: 26 PL intensity of complexes

Complex	λ_{max}	Intensity	Complex	λ_{max}	Intensity	Complex	λ_{max}	Intensity
14a	430	1514	16a	432	6745	20a	445	690
15a	469	947	16c	437	1858	20c	454	2282
14c	468	170	17a	439	4183	**21a**	**434**	**6379**
14d	469	163	**17c**	**506**	**302**	21c	465	1276
15c	453	1764						
15d	**432**	**3908**						

The **Table 26,** infers that among the complexes, **15d** of iridium complex and **17c** of platinum complex is highly photoluminescence.[12] On overall comparison, it was found that the cobalt (II) complexes to be highly luminescent. All the complexes having greater extensive conjugation are found to be more luminescent.

6.1.9. Cyclic Voltammtery

The cyclic voltammetry of the metal complexes depends upon the electron density of the metal and ligand. There is a change in potential (ie) shift in the oxidation and reduction potential of the wave. As the electron density of the system increase, which are

identified by increase in the potential shift, the energy storage efficiency may also increase. This can be studied in future work.

The overall redox behavior of corresponding metal complexes was shown in **fig (230-232).**

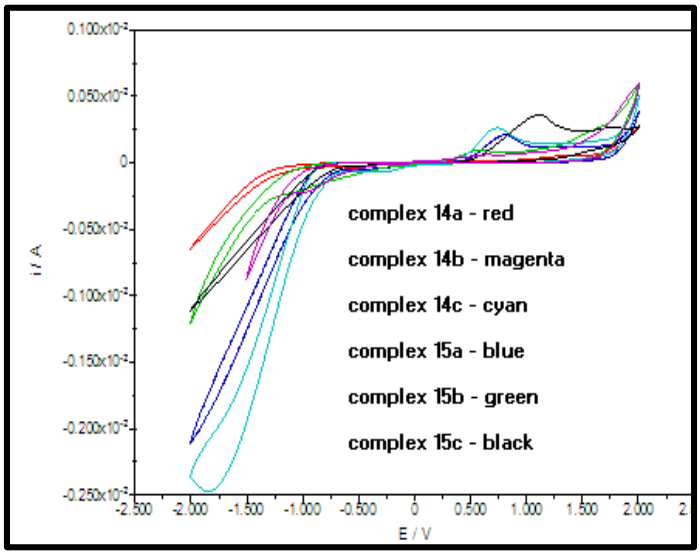

Fig 230 - Cyclic voltammtery of Ir(III) complexes

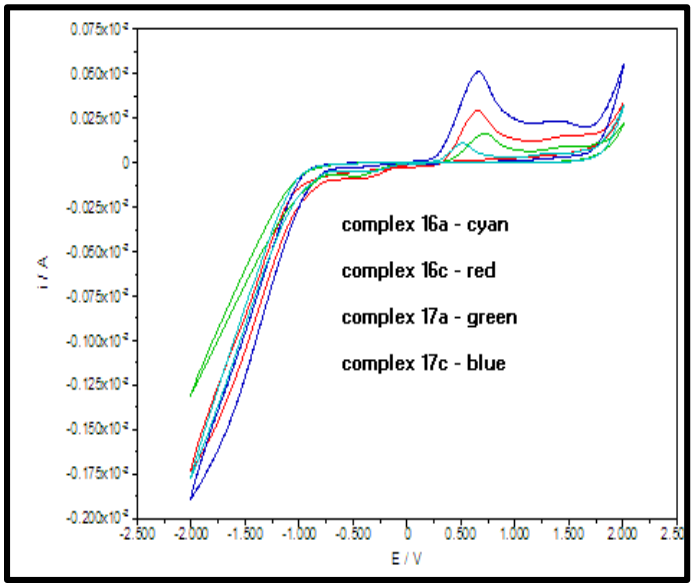

Fig 231 - Cyclic voltammtery of Pt(IV) complexes

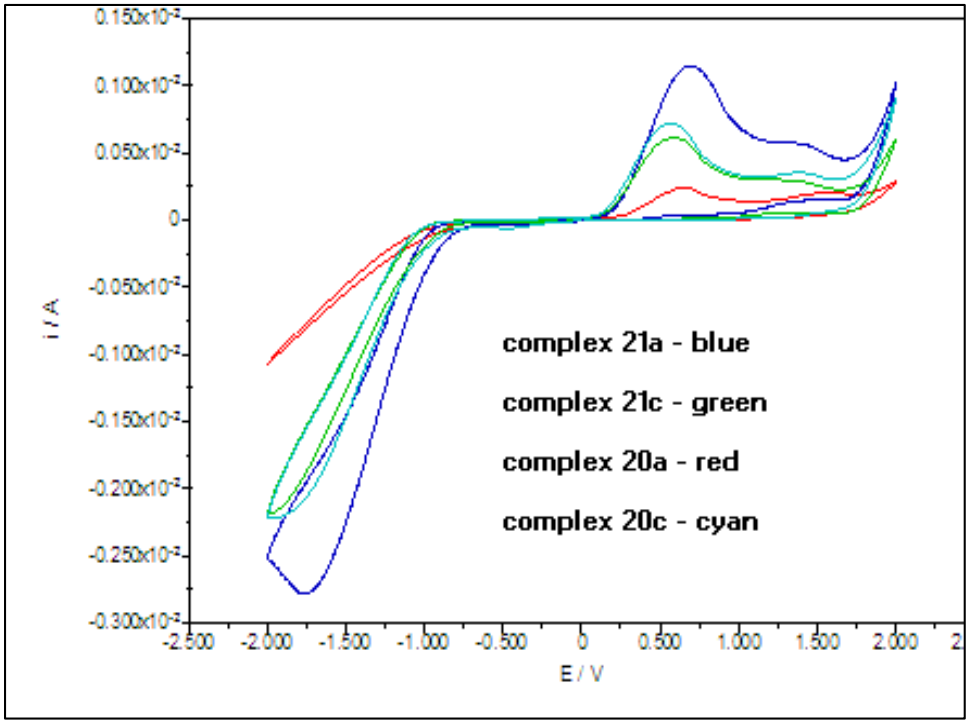

Fig 232 - Cyclic voltammtery of Co(II) complexes

HOMO, LUMO energy value of DFT studies and band energy[13] well coincides with that calculated from CV studies.

Compound	Oxidation Potential in volts	HOMO in eV		reduction Potential in volts	LUMO in eV		ΔE in eV		Band ganp	
		Cal.	Theor.		Cal.	Theor.	Cal.	Theor.	λ_{max}	E_g
Iridium(III) Complex (15c)	1.726	6.53	-7.01	-1.846	-3.0	-2.49	3.53	4.52	417	3.1
Cobalt (II) Complex (21c)	1.299	6.10	-6.84	-2.00	-2.8	-2.21	3.35	4.63	437	2.9

Emission, luminescence and cyclic voltammteric studies indicates that the iridium and cobalt complexes was acts as good OLED material.

References

1. P. Zhang, P. J. Sadler, *J. of Organomet. Chem*, **839**, 5-14 (2017).
2. S. H. van Rijt, P. J. Sadler, *Drug Discov Today*. **14,** 1089–1097 (2009).
3. U. Ndagi, N. Mhlongo, M. E Soliman, *Drug Des Devel Ther*, **11**, 599–616 (2017).
4. R. Bevernaegie, L. Marcelis, B. Elias, *Inorg. Chem*, ***57*** **(3)**, 1356–1367 (2018).
5. I. Kostova, *Recent Patents on Anti-Cancer Drug Discovery*, **1(1),** 1-22 **(**2006).
6. C. C. Konkankit , S. C. Marker , K. M. Knopf , J. J. Wilson .*Dalton Trans.,* **47(30)**, 9934-9974 (2018).
7. X. Y. Cui, Y. Ge, S. M. Tan, *J. Am. Chem. Soc*, ***140*** **(27),** 8448–8455 (2018).
8. C. Hong, T. J. Boggon, *Cancer cell*, **11**(3), 217-227 (2007).
9. G. M. R. Huey, W. Lindstrom, *J. of computational chemistry*, **30(16),** 2785-279, (2009).
10. G. Sathya Priyadarshini, R. Namitha, G. Selvi, *Int J Chem Sci*, **15(3),** 158 (2017).
11. M.H. Qi, G. F. Liu, *J. Phys. Chem. B*, **107(31)**, 7640–7646 (2003).
12. P. Petrova, R. Tomova, Bulgarian Chemical communications, 159-163 (2013).

Summary

The present work was aimed at the exploration of platinum group metal complexes as potent anticancer drugs and OLED material.

Chapter 1 dealt with the synthesis of the ligand substituted 4-methyl-2-(salicylidenehydrazino)quinoline **(11)** and substituted 4-methyl-2-(salicylidenethiosemicarbazino)quinoline **(13)** required for complexation with metals.

Accordingly the hydrazino and thiosemicarbazones were prepared from their potential precursor 4-methyl-2-chloro quinoline by reaction with hydrazine hydrate and thiosemicarbazide. The precursor 2-chloro-4-methyl quinoline was obtained by treating 2-hydroxy-4-methyl quinoline with $POCl_3$ which inturn was obtained by cyclisation of ethyl acetoacetate.

The ligands were then obtained by reacting hydrazone and thiosemicarbazone with salicyaldehyde respectively.

DFT studies were also carried out for the ligands in order to predict the mode of coordination sites to the metal salts.

Chapter II dealt with the synthesis of Ir(III) complexes with the ligands **(11)** and **(13)** respectively. The complexes were characterized using IR, NMR, UV, CV, TGA-DSC analysis. The results were also supported by the powedered XRD studies.

The DFT studies are well in line with the experimental characterization and confirmation. The mode of coordination is NNO mode.

Synthesis of Pt(IV) complexes were achieved by the reaction of substituted 4-methy-2-(salicylidenehydrazino)quinoline **(11)** and substituted 4-methy-2-(salicylidenethiosemicarbazino)quinoline **(13)** with K_2PtCl_6. After usual workup procedure, the complexes were characterized using IR, NMR, UV, CV, TGA and DFT. These are discussed in **chapter III.**

Chapter IV includes the synthesis and characterization of osmium (III) complexes by following the same experimental procedure. Hence the modes of coordination were found to be NNO which is different from the other platinum group metals. The difference noted in the spectral and analytical data was further confirmed by the changes noticed. From the results obtained from the theoretical studies.

Chapter V apart from the platinum group metals some series of reactions were carried out with Co(II) salt to obtain cobalt (II) complexes and the complexes were characterized using usual techniques.

Chapter VI involves the biological and photophysical studies on the synthesised complexes.

Antibacterial, antifungal, antioxidant, molecular docking, DNA cleavage and cytotoxic activity were studied for the selected ligands and the complexes. A comparison is made on the results obtained.

Photophysical studies such as emission, luminescence and cyclic voltammetry was carried out and the results obtained showed the complexes might acts as good OLED material.